Noise Reduction in Lidar Signals Using Interval-Thresholded Empirical Mode Decomposition

Kevin R. Leavor
email: kevin.leavor@gmail.com Ph: 757-728-6949
Co-Authors: M. Patrick McCormick, Neda Boyouk, Jia Su, Robert B. Lee III

Department of Atmospheric and Planetary Sciences
Hampton University, Hampton, VA 23668

6 June 2013

Outline

The Problem

Lidar requires a high signal-to-noise ratio to measure scattered laser pulses against the atmospheric and electronic backgrounds.

Noise Considerations

- Inversion process causes noise to become non-linear and non-stationary
- Sources of noise are difficult to completely eliminate.

Inadequate Solutions

- Statistical methods work against lidar's strengths by degrading resolution.
- Signal processing methods of denoising attempt to rebuild the signal instead of removing noise.

HU Lidar

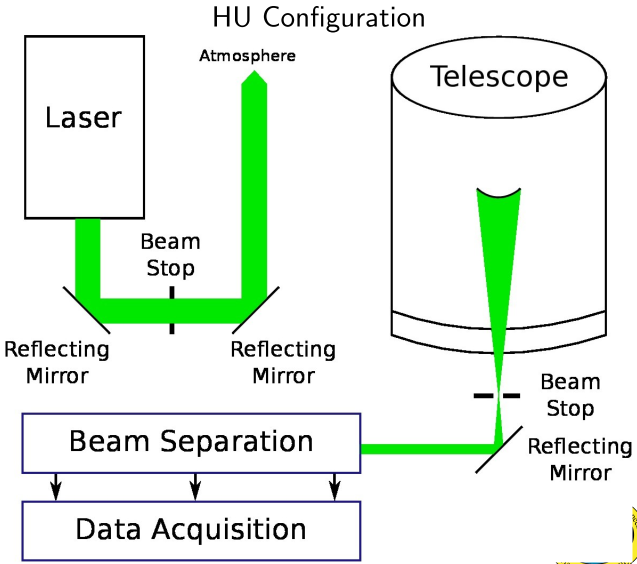
HU Configuration
Laser
Atmosphere
Telescope
Beam
Stop
Reflecting
Mirror
Reflecting
Mirror
Beam
Stop
Reflecting
Mirror
Beam Separation
Data Acquisition

HU Lidar

Lidar Equation

$$P(R) = C\left[\frac{O(R)}{R^2}\right]\beta(R)\exp\left\{-2\int_0^R \alpha(r)\,dr\right\}$$

[Fernald et al., 1972]

Performance - SNR Concerns

- Decreasing power with increasing range
- Decreasing scatterer densities with increasing range

Sources of Noise

- Poisson (Counting) Errors
  - Solar Background
  - Electrical/System noise (as above)

Inversion

Fernald Inversion (Aerosol Extinction/Backscatter) [Fernald et al., 1972; Klett, 1981; Sasano et al., 1985]

- Differential Equation solution to the lidar equation

$$\beta_a(R) = -\beta_m(R) + \frac{X(R)\exp\left\{-2\int_{R_0}^{R}[L_a(R)-L_m]\beta_m(r)\,dr\right\}}{\frac{X(R_0)}{\beta_a(R_0)+\beta_m(R_0)} - 2\int_{R_0}^{R} L_a(r)X(r)T(R_0,r)}$$

Limitations

- Requires a reference altitude of known backscatter coefficient or backscatter ratio. (1%Error $\rightarrow x10$ [Russell et al., 1979])
- Noise becomes a non-stationary with a near-linear dependency on range. (Logarithmic R^2 dependency [Klett, 1981])
- Integration is more stable in the backwards direction than forward [Sasano et al., 1985]

Inversion

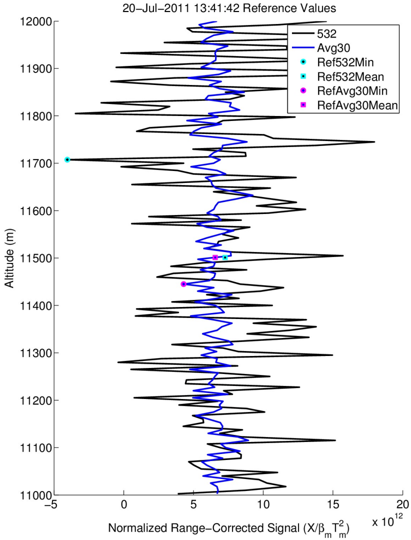
20–Jul–2011 13:41:42 Reference Values
532
Avg30
Ref532Min
Ref532Mean
RefAvg30Min
RefAvg30Mean
Altitude (m)
Normalized Range–Corrected Signal (X/β_m T^2_m)
x 10^12
20–Jul–2011 13:41:42 Reference Values
532
CIIT
Ref532Min
Ref532Mean
RefCIITMin
RefCIITMean
Altitude (m)
Normalized Range–Corrected Signal (X/β_m T^2_m)
x 10^12

Inversion

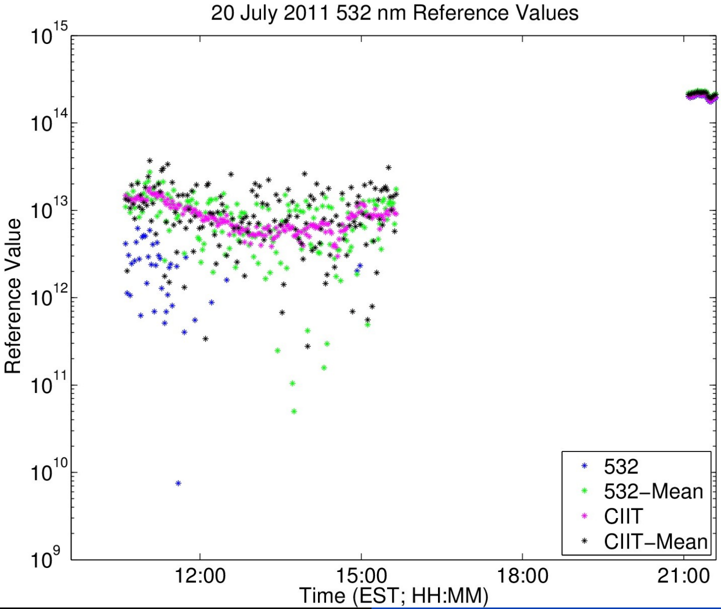
20 July 2011 532 nm Reference Values
Reference Value
Time (EST; HH:MM)
10^15
10^14
10^13
10^12
10^11
10^10
10^9
12:00
15:00
18:00
21:00
532
532−Mean
CIIT
CIIT−Mean

EMD

20 July 2011
532 nm Signal EMD

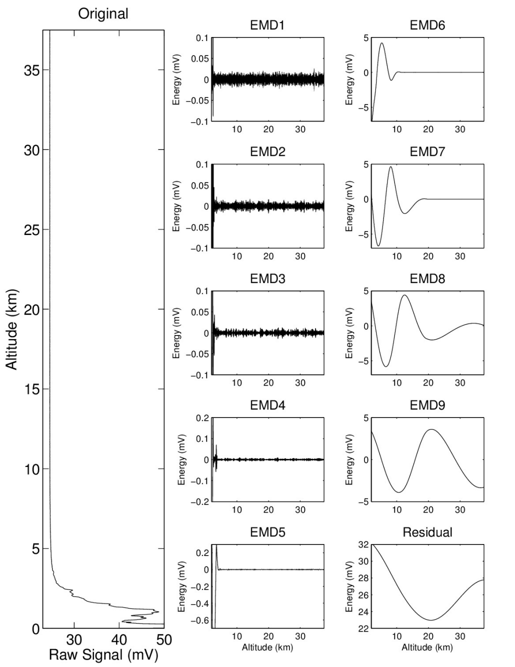

EMD

EMD Sifting Process

Produce basis functions via an intuitive, direct, *a posteriori*, and adaptive technique. [Huang et al., 1998]

Assumptions

- The signal has at least two extrema (Maximum + Minimum)
- The characteristic time scale is defined by the time lapse between the extrema
- If the data are devoid of extrema, containing only inflection points, differentiation will reveal extrema.

Stopping Criteria

$$\mathrm{SD} = \sum_{t=0}^{T} \left[\frac{\left| h_{1(k-1)}(t) - h_{1k}(t) \right|^2}{h_{1(k-1)}^2(t)} \right]$$

EMD

EMD Denoising

- Current application to lidar is rudimentary [Liu et al., 2008; Wu et al., 2006; Zhang et al., 2010; Zhao and Colony, 2001].
  - The first set of IMFs are discarded as completely noise.
    - Cutoff may be arbitrary or determined via power spectra.
  - Filtering (Savitzky-Golay) may be applied instead of directly discarding IMFs.
  - Direct thresholding as in wavelet has also been applied [Boudraa, 2004; Gong et al., 2011].

Limitations

- Discarding IMFs can lead to loss of structure or introduction of oscillations.
  - Reconstructing a non-periodic signal with periodic components.
- Direct thresholding on continuous IMFs introduces errors.

Methods

EMD Thresholding [Donoho and Johnstone, 1994; Kopsinis and McLaughlin, 2008]

- Each IMF is denoised using a thresholding technique.
  - Thresholding is applied based on the interval between zero crossings
- Signal is suppressed by a thresholding parameter (τ) if outside $\pm\tau$, and zeroed otherwise (Soft-T).
  - Similar to wavelet thresholding; Interval scaled accordingly.
  - Since IMFs are continuous function, any extrema outside the threshold preserves the points inside the threshold (Interval Thresholding) [Kopsinis and McLaughlin, 2008].
- Denoised signal is generated from the sum of the denoised IMFs. ($S^*(t) = \sum c_i^*(t)$)
  - Note: $S(t) = \sum c_i(t)$.
- Preserves major, yet highly localized, features in noise (high frequency) components.

EMD Thresholding

EMD-CIIT [Kopsinis and McLaughlin, 2009]

- EMD acts as a dyadic filter, so first IMFs contain almost all of the noise [Flandrin et al., 2004].
- Virtually resample the signal by randomly circulating the 1^{st} noise-dominant IMF with a reconstruction from the remaining denoised IMFs. **Think Bootstrapping!**
- Perform EMD on each resample and average for a potentially better signal estimate.
  - Filter using wavelet before permutation since first IMF might contain information (thin aerosol/cloud layers).

Test Cases

Modeled Signal

- Generate base signal using lidar equation and normalize to maximum of 100.
- Only include molecular scattering from U. S. Standard Atmosphere 1976 [NOAA, 1976]
- 3 Gaussians added to simulate aerosol/cloud features
- Add noise with $\mu = 0$, $\sigma = 0.1\% \max[P(R)]$

Measured Signal

- 532 nm signal from 20 July 2011 at 13:41:42 EST
- 20 July 2011 1064 and 532 nm Aerosol Extinction Coefficients
- 19–20 April 2012 Raman Temperature Profiles
- 21 April 2012 1064 and 532 nm PBL Heights

Test Cases

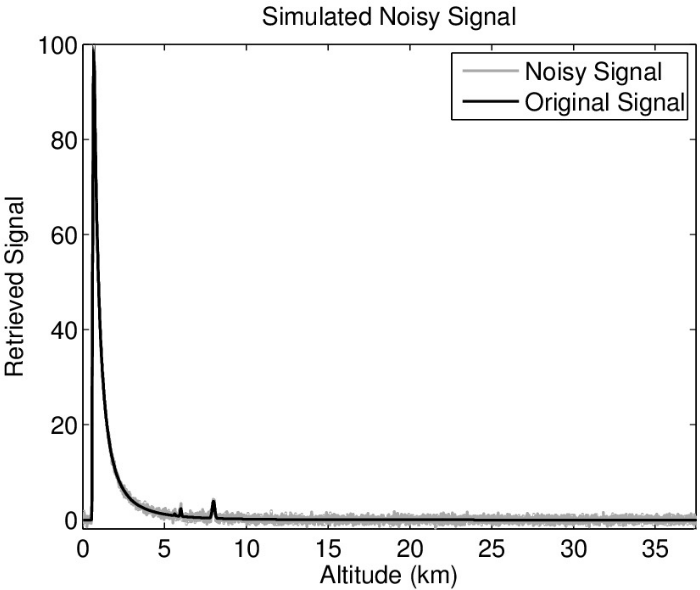
Simulated Noisy Signal
Noisy Signal
Original Signal
Retrieved Signal
100
80
60
40
20
0
0
5
10
15
20
25
30
35
Altitude (km)

Test Cases

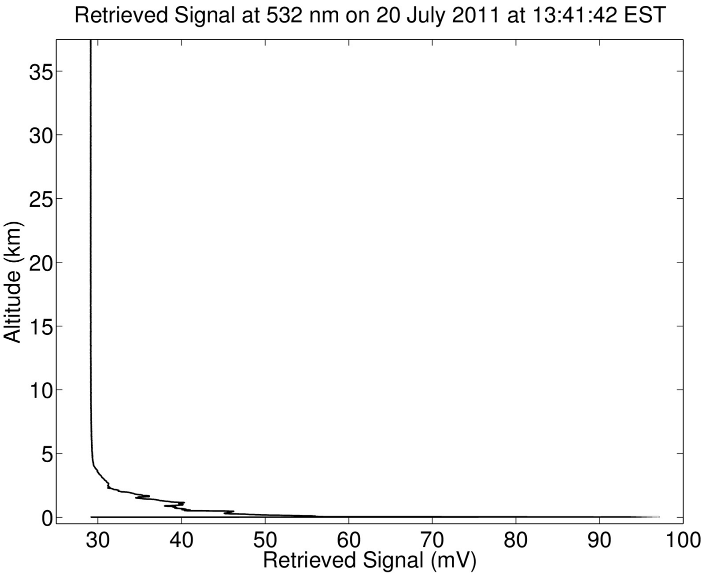
Retrieved Signal at 532 nm on 20 July 2011 at 13:41:42 EST
Altitude (km)
35
30
25
20
15
10
5
0
30
40
50
60
70
80
90
100
Retrieved Signal (mV)

Test Cases

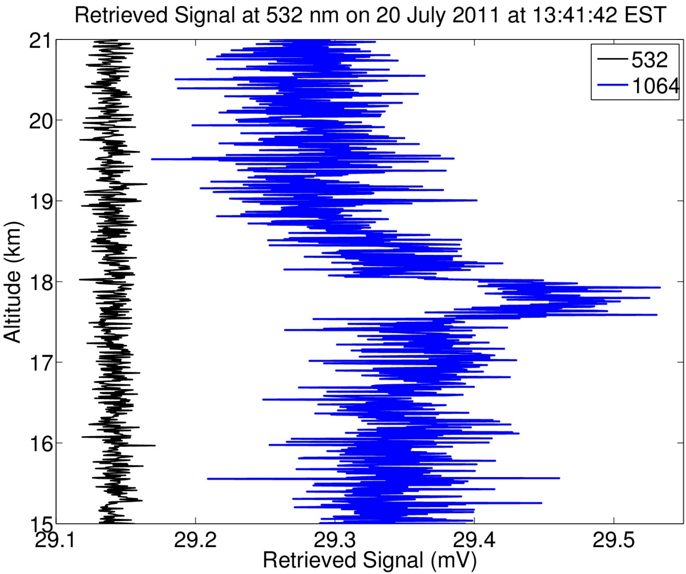
Retrieved Signal at 532 nm on 20 July 2011 at 13:41:42 EST
532
1064
Altitude (km)
Retrieved Signal (mV)
21
20
19
18
17
16
15
29.1
29.2
29.3
29.4
29.5

Results - Simulated Signal Tests

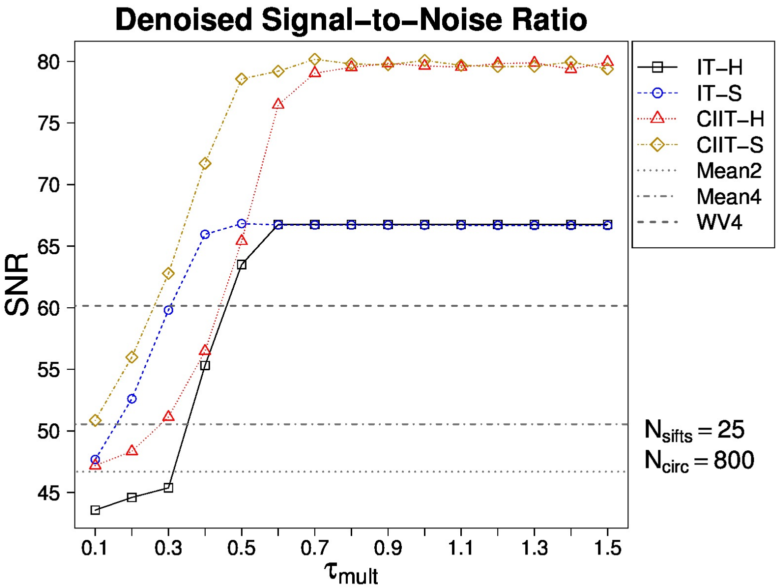

Results - Simulated Signal Tests

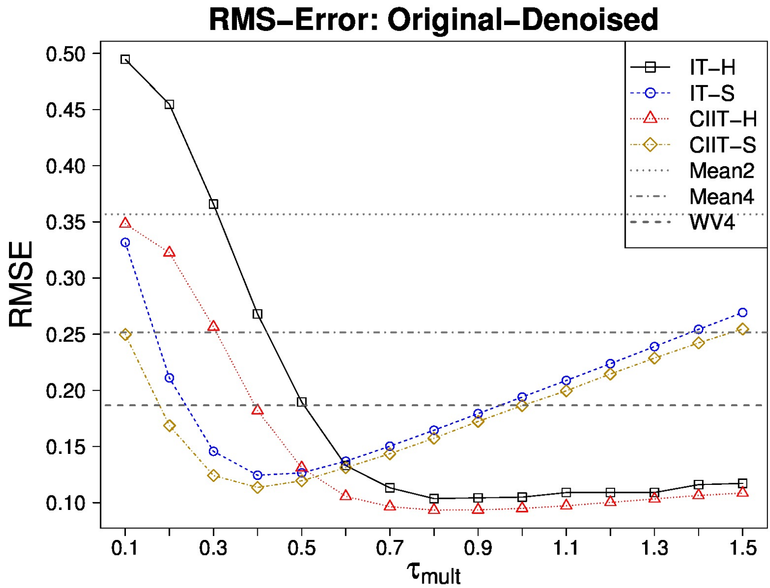

Results - Simulated Signal Tests

2-Sample Anderson-Darling p-Values: Injected Noise vs. Traditionally Removed Noise for Modeled Signal

	Technique				
	Mean2	**Mean4**	**WV4**	**WV6**	**WV8**
p_{AD}	0.00	0.00	0.09	0.12	0.12

2-Sample Anderson-Darling

- Hard-Thresholded EMD-IT passes for $\tau_{\text{mult}} \in [0.5, 1.5]$
  - Some dependence on N_{sifts} with best results between 15–17
- Soft-Thresholded EMD-IT passes beginning at $\tau_{\text{mult}} = 0.4$ to variably between 0.5–0.9.
- Hard-Thresholded EMD-CIIT passes unifromly from $\tau_{\text{mult}} \in [0.6, 1.5]$
- Soft-Thresholded EMD-CIIT passes from $\tau_{\text{mult}} = 0.4$ to 1.1–1.3.
  - No significant dependence on N_{sifts}. Significant gains from N_{circ} converging quickly after 80.

Results - 532 nm Signal Tests

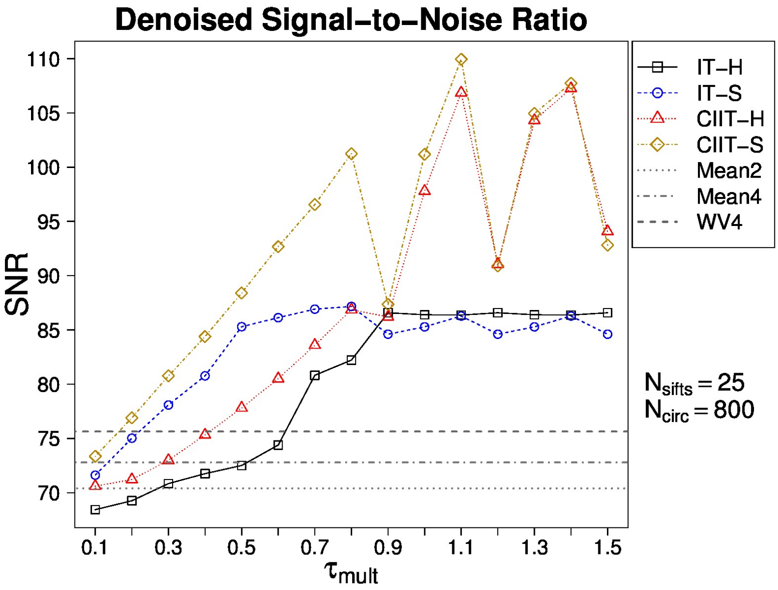

Results - 532 nm Signal Tests

1-Sample p-Values: Injected Noise vs. Traditionally Removed Noise for 20 July 2012 532 nm Signal

	Technique				
	Mean2	**Mean4**	**WV4**	**WV6**	**WV8**
p_{AD}	0	0	1.330×10^{-20}	9.412×10^{-18}	6.446×10^{-12}
p_{SW}	3.701×10^{-90}	5.492×10^{-90}	1.207×10^{-22}	6.350×10^{-22}	1.453×10^{-18}

1-Sample Anderson-Darling and Shapiro-Wilk Tests

- Hard-Thresholded EMD-IT has no consistent values between tests.
- Soft-Thresholded EMD-IT passes consistently for $\tau_{\text{mult}} = 0.4$.
- Hard-Thresholded EMD-CIIT passes unifromly from $\tau_{\text{mult}} \geq 0.7$ and $N_{\text{sifts}} \geq 15$
- Soft-Thresholded EMD-CIIT passes from $\tau_{\text{mult}} \in [0.3, 0.4]$.

Results - 20 July 2011 Aerosol Extinction

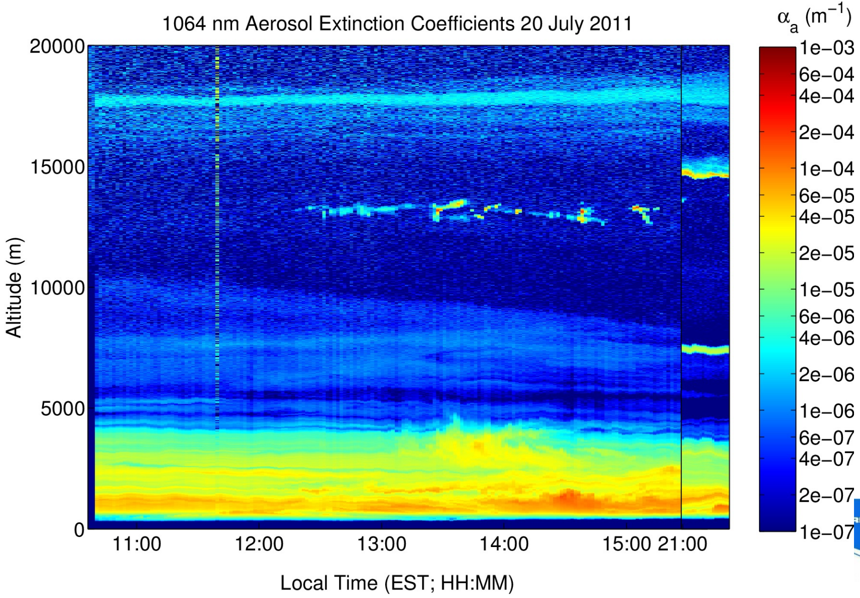

Results - 20 July 2011 Aerosol Extinction

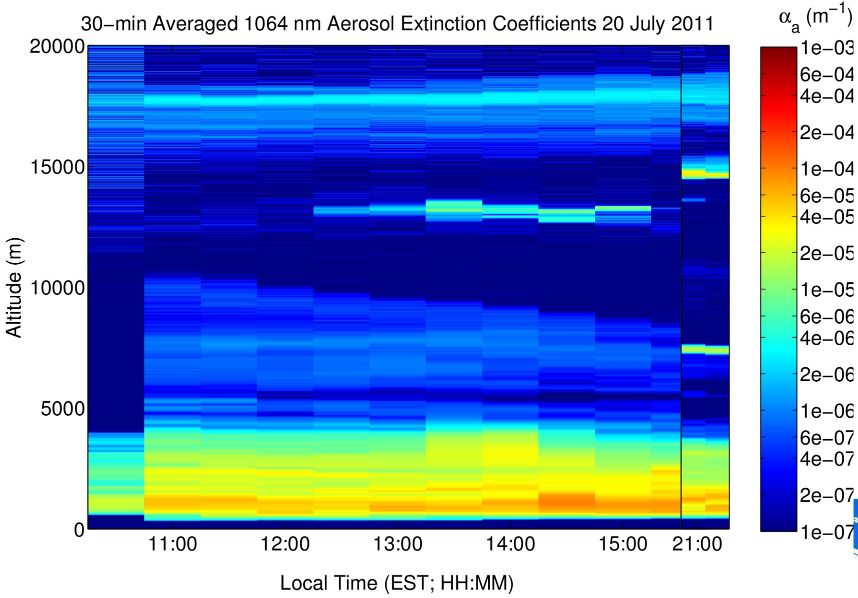

Results - 20 July 2011 Aerosol Extinction

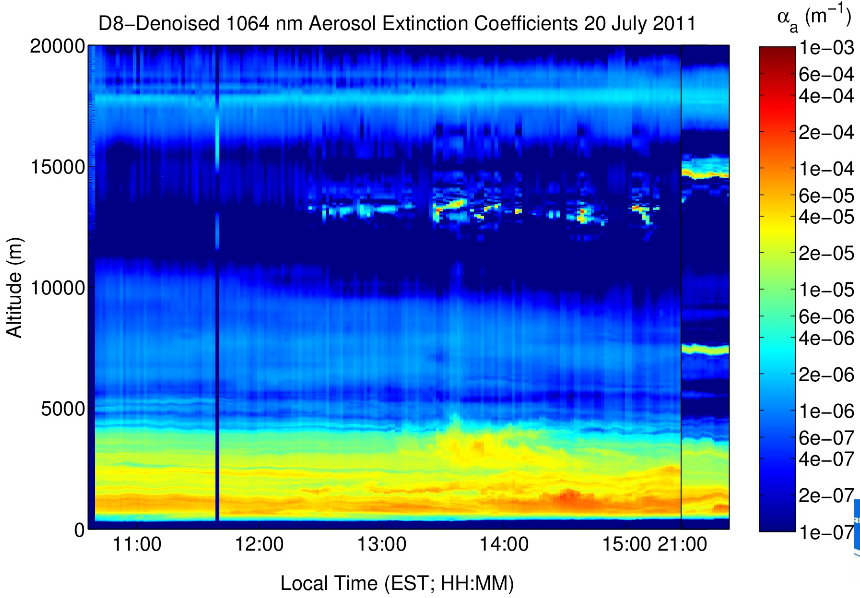

Results - 20 July 2011 Aerosol Extinction

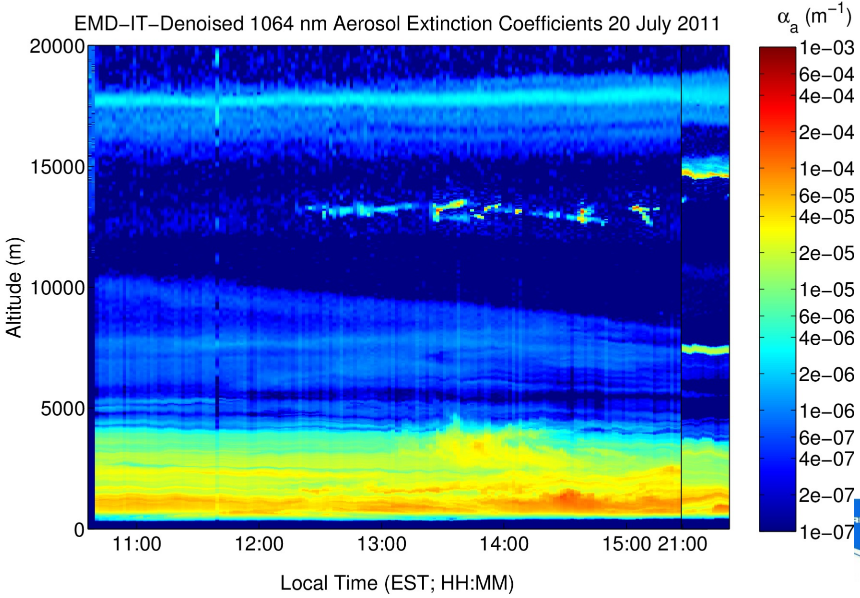

Results - 20 July 2011 Aerosol Extinction

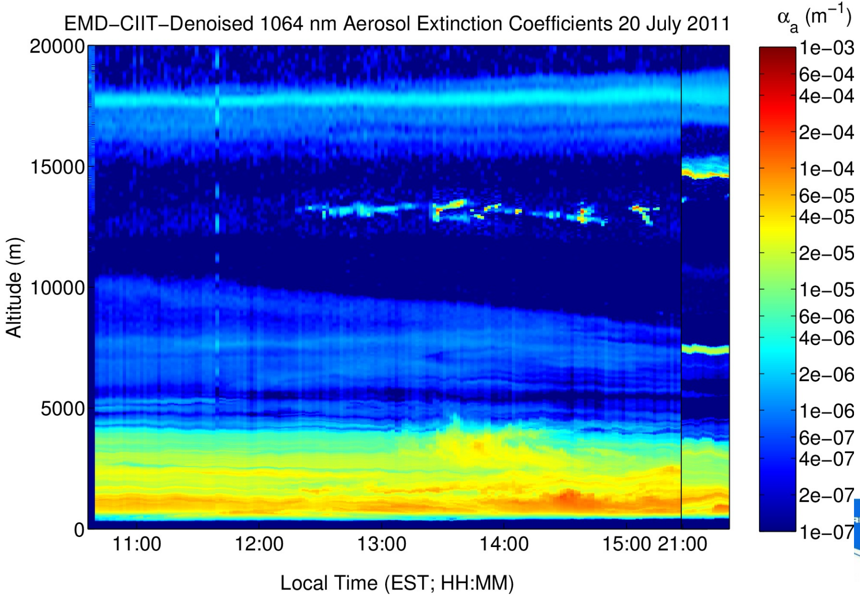

Results - 20 July 2011 Aerosol Extinction

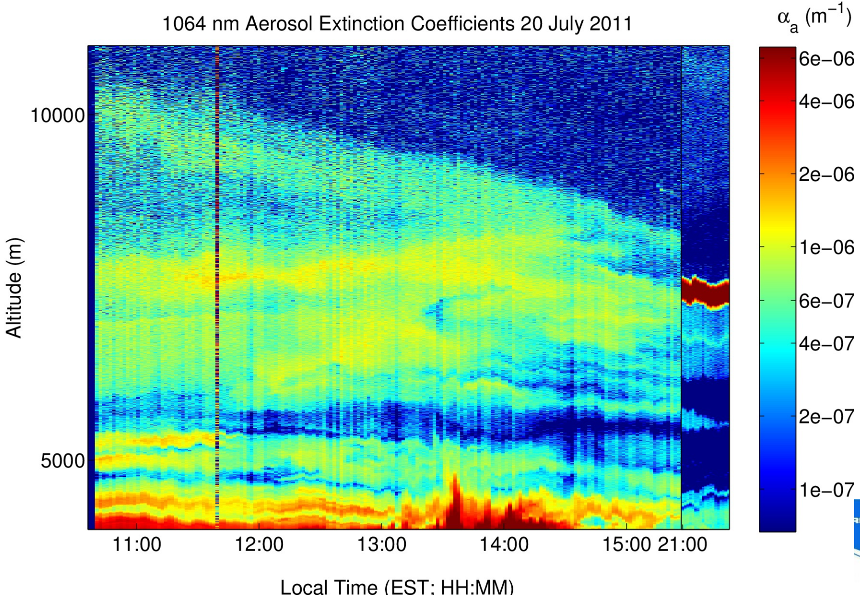

Results - 20 July 2011 Aerosol Extinction

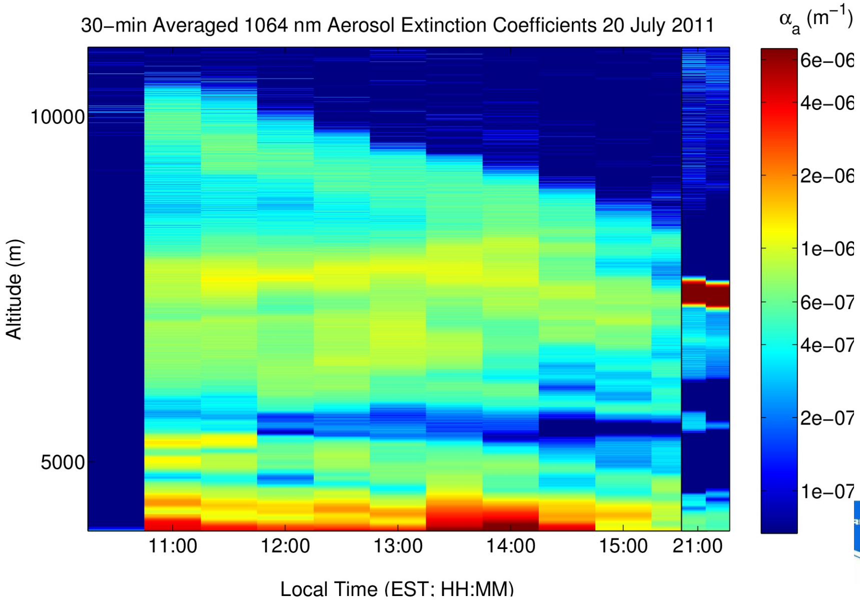

Results - 20 July 2011 Aerosol Extinction

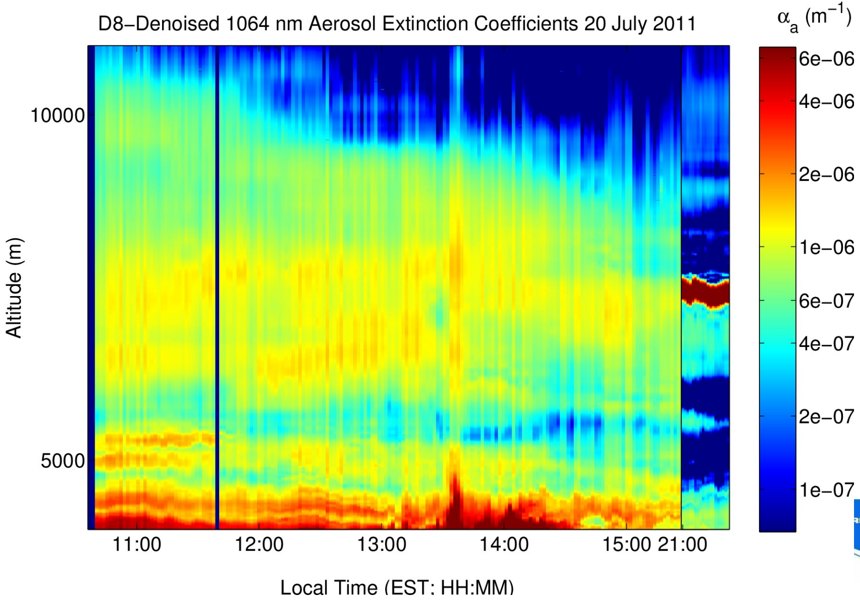

Results - 20 July 2011 Aerosol Extinction

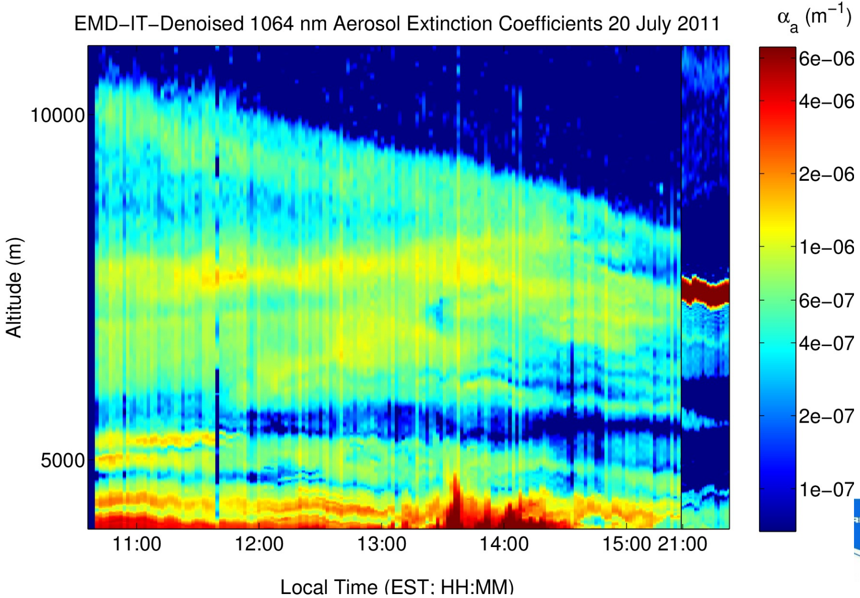

Results - 20 July 2011 Aerosol Extinction

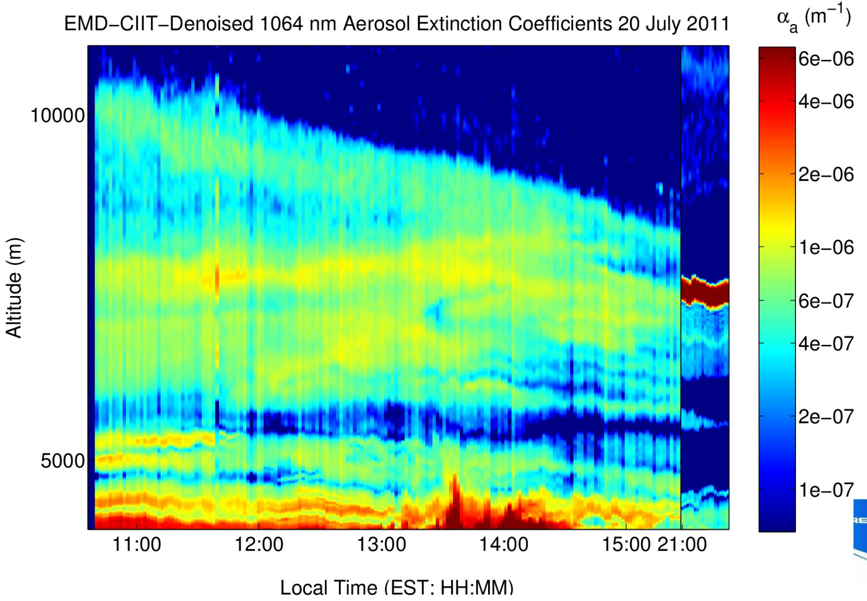

Results - 20 July 2011 Aerosol Extinction

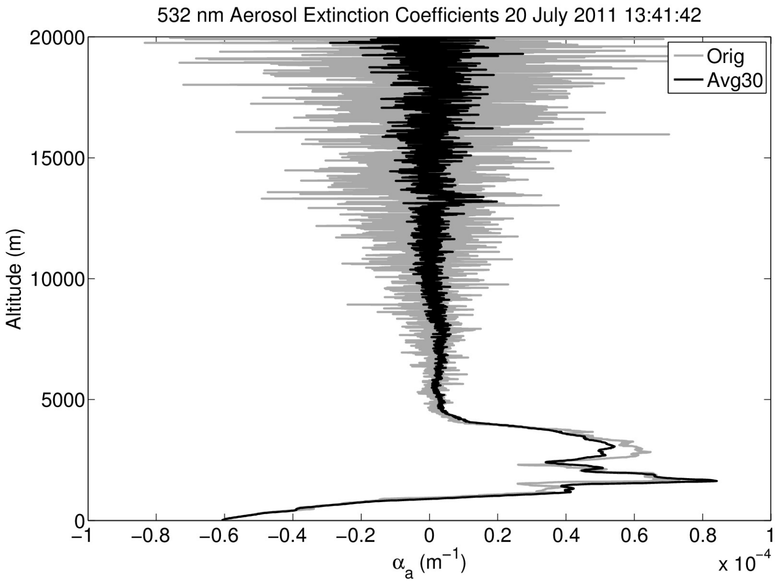

Results - 20 July 2011 Aerosol Extinction

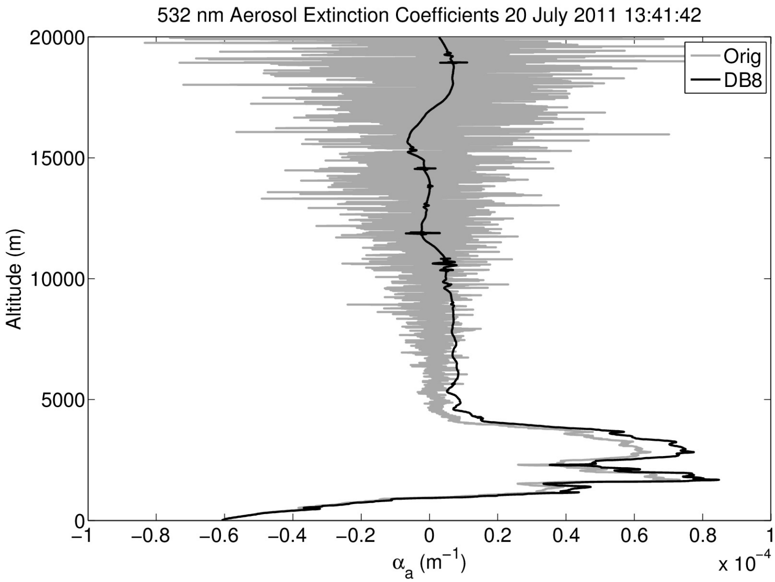

Results - 20 July 2011 Aerosol Extinction

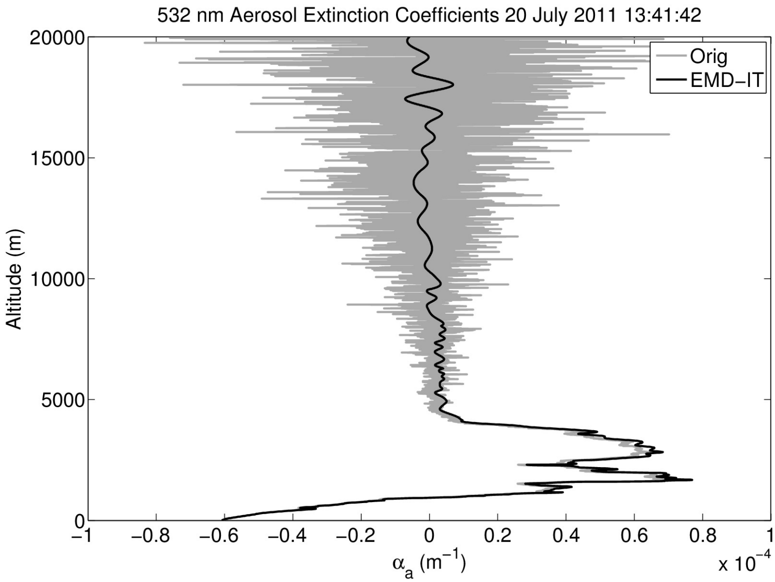

Results - 20 July 2011 Aerosol Extinction

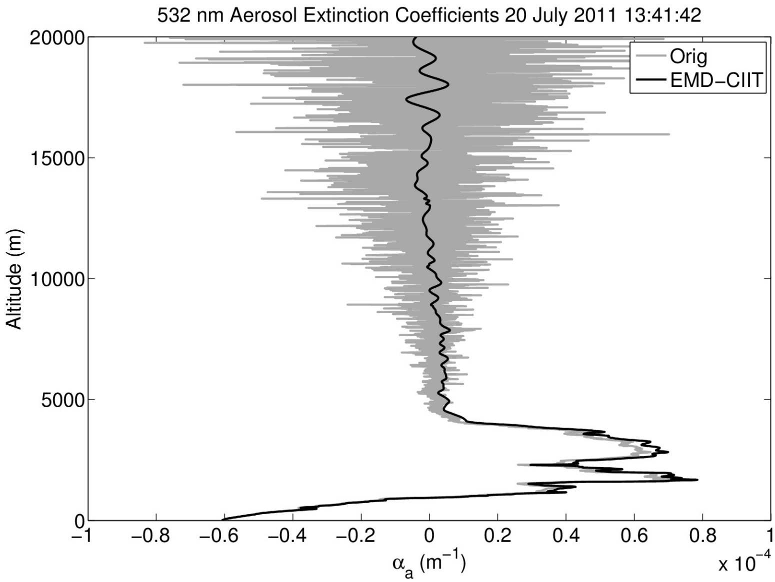

Results - 20 July 2011 Aerosol Extinction

Noise-Reduction Statistics for Denoised 1064 nm Range-Corrected Signal and Aerosol Extinction Coefficients on 20 July 2011 13:41:42

Method	σ_X	$\%_{Err,X}$	σ_α	$\%_{Err,\alpha}$	$r_{full,X}$	$r_{full,\alpha}$	$r_{strat,X}$	$r_{strat,\alpha}$
Base	1.71e+06	32.36%	5.67e-07	46.27%	1.0000	1.0000	1.0000	1.0000
Avg15	—	—	—	—	0.9883	0.9838	0.8594	0.8528
Avg30	—	—	—	—	0.9764	0.9688	0.8355	0.8277
Avg60	—	—	—	—	0.9703	0.9641	0.8138	0.8043
DB4	3.52e+05	5.87%	1.08e-07	7.86%	0.9969	0.9950	0.7896	0.7730
DB6	3.72e+05	8.80%	1.60e-07	15.98%	0.9968	0.9946	0.7691	0.7587
DB8	2.11e+05	4.39%	1.27e-07	10.14%	0.9967	0.9946	0.7590	0.7444
IT	3.65e+05	7.04%	1.20e-07	9.85%	0.9972	0.9955	0.8100	0.8009
CIIT	2.73e+05	5.19%	9.21e-08	7.53%	0.9972	0.9955	0.8128	0.8038

1. EMD performs at least as well as Wavelet noise reduction for overall signal
2. EMD outperforms wavelet and is comparable to long temporal averages for the stratospheric layer.

Results - 20 July 2011 Aerosol Extinction

Noise-Reduction Statistics for Denoised 532 nm Range-Corrected Signal and Aerosol Extinction Coefficients on 20 July 2011 13:41:42

Method	σ_X	$\%_{Err,X}$	σ_α	$\%_{Err,\alpha}$	$r_{full,X}$	$r_{full,\alpha}$	$r_{strat,X}$	$r_{strat,\alpha}$
Base	1.51e+06	21.60%	4.48e-07	29.10%	1.0000	1.0000	1.0000	1.0000
Avg15	—	—	—	—	0.9906	0.9879	0.7971	0.7934
Avg30	—	—	—	—	0.9375	0.9299	0.7075	0.7018
Avg60	—	—	—	—	0.9777	0.9722	0.7733	0.7691
DB4	2.59e+05	3.51%	5.70e-08	3.68%	0.9976	0.9963	0.6737	0.6671
DB6	1.96e+05	3.10%	5.37e-08	3.90%	0.9975	0.9962	0.6571	0.6539
DB8	2.60e+05	3.99%	6.62e-08	4.28%	0.9974	0.9959	0.6447	0.6383
IT	3.67e+05	5.27%	1.17e-07	7.66%	0.9978	0.9968	0.7462	0.7414
CIIT	2.95e+05	4.24%	7.75e-08	5.03%	0.9979	0.9968	0.7422	0.7369

1. EMD (esp. CIIT) performs comparably to wavelet in reducing signal σ
2. EMD outperforms wavelet and is comparable to long temporal averages for the stratospheric layer.
    - Particularly true for stratospheric layer.

Conclusion I

- Appropriate values for EMD-based denoising have been determined
  - $\tau_{\text{mult}} \in [0.3, 0.5]$ for Soft Thresholding
  - $\tau_{\text{mult}} \in [0.7, 1.1]$ for Hard Thresholding
  - N_{sifts} only significant for IT, ≈ 16 ideal.
  - Small N_{circ} for CIIT shows significant benefits (< 100). More siftings provides smoother signal.
- EMD-based denoising performs at least as well as traditional techniques
  - Higher SNR
  - Lower errors
  - Higher resolution than averaging and wavelet.
- EMD-based denoising introduces fewer artifacts into the resulting signal

Conclusion II

- Offers potentially large benefits to incredibly low SNR signals when combined with averaging techniques
  - Reduces the number of averaging bins required.
- Offers the least error in removing significant physical signal components.
- Still significant work for optimizing the technique to varying levels of signal SNR.
  - e.g. Raman Temperature vs. 532 nm Extinction vs. 1064 nm Extinction
  - Applications to other atmospheric measurements worth exploring.

Acknowledgments

- Advisor: M. Patrick McCormick
- Committee: Robert Loughman, Michael Hill, Ali Omar
- Neda Boyouk and Jasper Lewis for PBL and Lidar Processing Contributions
- Lidar Team: Jia Su, Liqiao Lei, Robert Lee, Sufia Khatun
- NOAA-CREST, Army Research Lab, NSF-CREST for funding and support

BACKUP SLIDES

Selected References I

Arshinov, Y. F., S. M. Bobrovnikov, V. E. Zuev, and V. M. Mitev, 1983: Atmospheric temperature measurements using a pure rotational raman lidar. *Appl. Opt.*, **22 (19)**, 2984–2990, doi:10.1364/AO.22.002984.

Behrendt, A., 2005: *Lidar: Range-Resolved Optical Remote Sensing of the Atmosphere (Springer Series in Optical Sciences)*, chap. 10: Temperature Measurements with Lidar, 273–305. Springer, New York, NY.

Behrendt, A. and J. Reichardt, 2000: Atmospheric temperature profiling in the presence of clouds with a pure rotational raman lidar by use of an interference-filter-based polychromator. *Appl. Opt.*, **39 (9)**, 1372–1378, doi:10.1364/AO.39.001372.

Boudraa, A. O., 2004: EMD-Based Signal Noise Reduction. *Int. J. of Sig. Proc.*, **1 (1)**, 33–37.

Brooks, I. M., 2003: Finding Boundary Layer Top: Application of a Wavelet Covariance Transform to Lidar Backscatter Profiles. *J. Atmos. Ocean. Tech.*, **20**, 1092–1105.

Cohen, A., J. A. Cooney, and K. N. Geller, 1976: Atmospheric temperature profiles from lidar measurements of rotational raman and elastic scattering. *Appl. Opt.*, **15 (11)**, 2896–2901, doi:10.1364/AO.15.002896.

Daubechies, I., 1988: Orthonormal bases of compactly supported wavelets. *Communications on Pure and Applied Mathematics*, **41 (7)**, 909–996, doi:10.1002/cpa.3160410705.

Daubechies, I., 1992: *Ten lectures on wavelets*. Society for Industrial and Applied Mathematics, Philadelphia, Pa.

Davis, K., N. Gamage, C. Hagelberg, C. Kiemle, D. Lenschow, and P. Sullivan, 2000: An objective method for deriving atmospheric structure from airborne lidar observations. *J. Atmos. Ocean. Tech.*, **17 (11)**, 1455.

Donoho, D. L., 1995: De-Noising by Soft-Thresholding. *IEEE Trans. on Info. Theory*, **41 (3)**, 613–627.

Donoho, D. L. and I. M. Johnstone, 1994: Ideal spatial adaptation by wavelet shrinkage. *Biometrika*, **81 (3)**, 425–455.

Fang, H.-T. and D.-S. Huang, 2004: Noise reduction in lidar signal based on discrete wavelet transform. *Optics Communications*, **233 (13)**, 67 – 76, doi:10.1016/j.optcom.2004.01.017.

Fernald, F. G., B. M. Herman, and J. A. Reagan, 1972: Determination of Aerosol Height Distributions by Lidar. *J. Appl. Meteo.*, **11**, 482–489.

Selected References II

Fiocco, G. and L. D. Smullin, 1963: Detection of Scattering Layers in the Upper Atmosphere (60-140 km) by Optical Radar. *Nature*, **199**, 1275–1276.

Flandrin, P., G. Rilling, and P. Gonçalvés, 2004: Empirical Mode Decomposition as a Filter Bank. *IEEE Sig. Proc. Lett.*, **11 (2)**, 112–114.

Gong, W., J. Li, F. Mao, and J. Zhang, 2011: Comparison of simultaneous signals obtained from a dual-field-of-view lidar andits application to noise reduction based on empirical mode decomposition. *Chin. Opt. Lett.*, **9 (5)**, 050101.

Huang, N. E., et al., 1998: The empirical mode decomposition and the Hilbert spectrum for nonlinear and non-stationary time series analysis. *Proc. R. Soc. Lond. A*, **454**, 903–995.

Klett, J. D., 1981: Stable analytical inversion solution for processing lidar returns. *Appl. Opt.*, **20 (2)**, 211–220.

Kopsinis, Y. and S. McLaughlin, 2008: Empirical mode decomposition based soft-thresholding. *Proc. 16th Eur. Sig. Process. Conf. (EUSIPCO)*, Lausanne, Switzerland, 42–47.

Kopsinis, Y. and S. McLaughlin, 2009: Development of EMD-Based Denoising Methods Inspired by Wavelet Thresholding. *IEEE Trans. on Sig. Proc.*, **57 (4)**, 1351–1362.

Lewis, J., E. J. Welton, L. R. Belcher, and Mplnet Team, 2011: Improved Boundary Layer and Cloud Heights from the NASA Micro Pulse Lidar Network (MPLNET). *AGU Fall Meeting Abstracts*, C354.

Liu, Z.-D., J. guo Liu, Y. huai Lu, X. song Zhao, S. hua Huang, W. wei Feng, and F. gang Xiao, 2008: De-noising lidar signal based on emd method. *Opto-Elec. Eng.*, **2008-06**.

McCormick, M. P. and K. R. Leavor, 2013: Active lidar remote sensing. *Aerosol Remote Sensing*, J. Lenoble, L. Remer, and D. Tanr, Eds., Springer Berlin Heidelberg, 283–313, doi:10.1007/978-3-642-17725-5_10, URL http://dx.doi.org/10.1007/978-3-642-17725-5_10.

McCormick, P. D., S. K. Poultney, U. van Wijk, C. O. Alley, and R. T. Bettinger, 1966: Backscattering from the Upper Atmosphere (75-160 km) detected by Optical Radar. *Nature*, **209**, 798–799.

NOAA, 1976: *U. S. Standard Atmosphere, 1976*, Vol. NOAA-S/T 76-1562. National Oceanic and Atmospheric Administration, 227 pp.

Selected References III

Russell, P. B., T. J. Swissler, and M. P. McCormick, 1979: Methodology for error analysis and simulation of lidar aerosol measurements. *Appl. Opt.*, **18 (22)**, 3783–3797.

Sasano, Y., E. V. Browell, and S. Ismail, 1985: Error caused by using a constant extinction/backscattering ratio in the lidar solution. *Appl Opt*, **24 (22)**, 3929–3932.

Wandinger, U., 2005: *Lidar: Range-Resolved Optical Remote Sensing of the Atmosphere (Springer Series in Optical Sciences)*, chap. 9: Raman Lidar, 241–271. Springer, New York, NY.

Wu, S., Z. Liu, and B. Liu, 2006: Enhancement of lidar backscatters signal-to-noise ratio using empirical mode decomposition method. *Optics Communications*, **267 (1)**, 137 – 144, doi:10.1016/j.optcom.2006.05.069.

Zhang, Y., X. Ma, D. Hua, Y. Cui, and L. Sui, 2010: An emd-based denoising method for lidar signal. *3rd International Congress on Image and Signal Processing (CISP)*, Yantai, China, 4016–4019.

Zhao, J. and R. Colony, 2001: Study on the effects of abnormal events to empirical mode de-composition method and the removal method for abnormal signal. *J. Ocean Uni. Qingdao*, **31 (6)**, 805–814.

EMD

Empirical Mode Decomposition [Huang et al., 1998]

- Decompose signal into **Intrinsic Mode Functions** (IMFs)
    - Functions whose local extrema differ from the total number of zero crossings by at most 1, and the mean value of an envelope enclosing those maxima and minima is 0.
- Sifting Process
    1. Cubic spline interpolate through maxima and minima to create two envelopes.
    2. Subtract mean of the envelopes from the signal and test result for IMF criteria. ($h_{1,1} = S(t) - m_{1,1}$)
    3. Algorithm continues until result is an IMF. ($c_1 = h_{1,n}$)
    4. c_1 is subtracted from $S(t)$ and the process continues on the remainder r_1.
    5. Process stops when r_n is an IMF or cannot be sifted into an IMF.
- IMFs represent (instantaneous) frequency components of the signal.

Results - 19–20 April 2012 Temperature

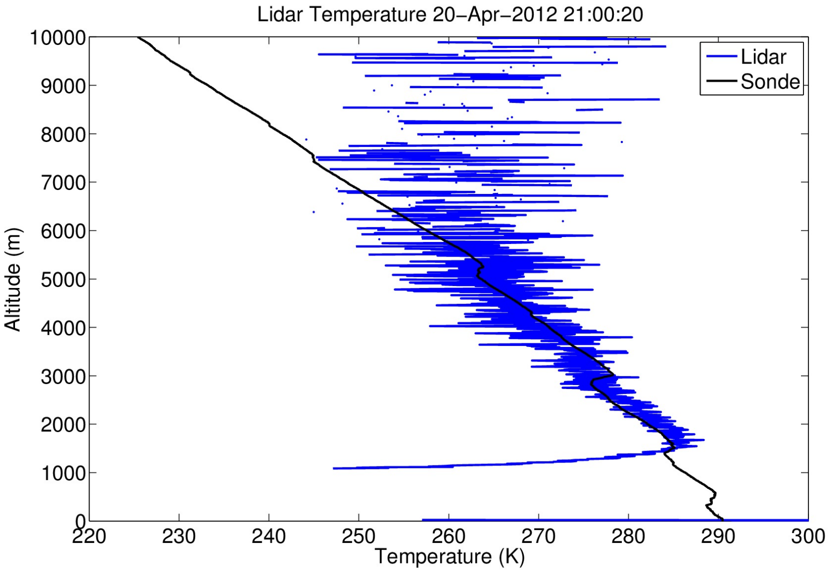

Results - 19–20 April 2012 Temperature

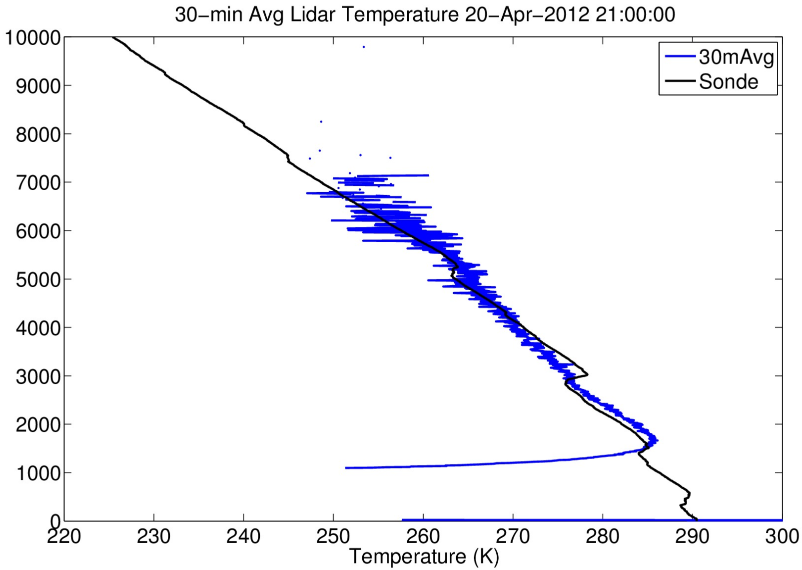

Results - 19–20 April 2012 Temperature

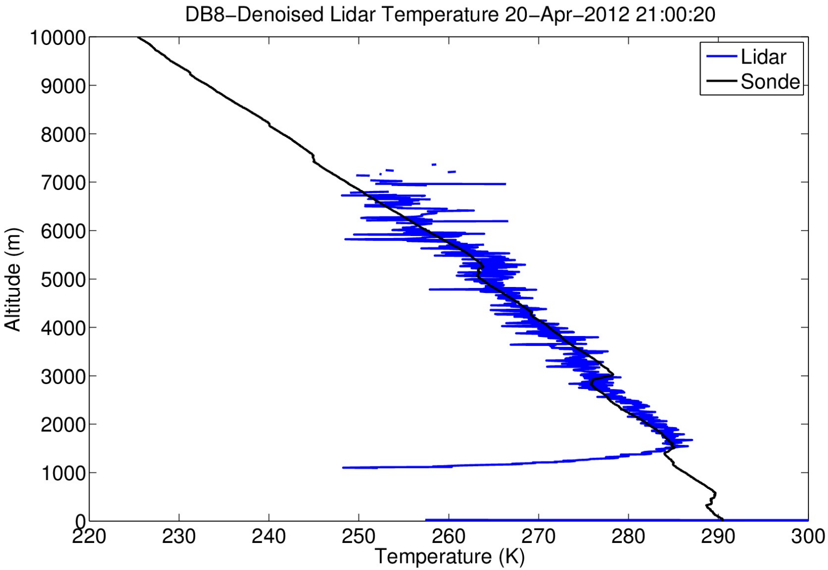

Results - 19–20 April 2012 Temperature

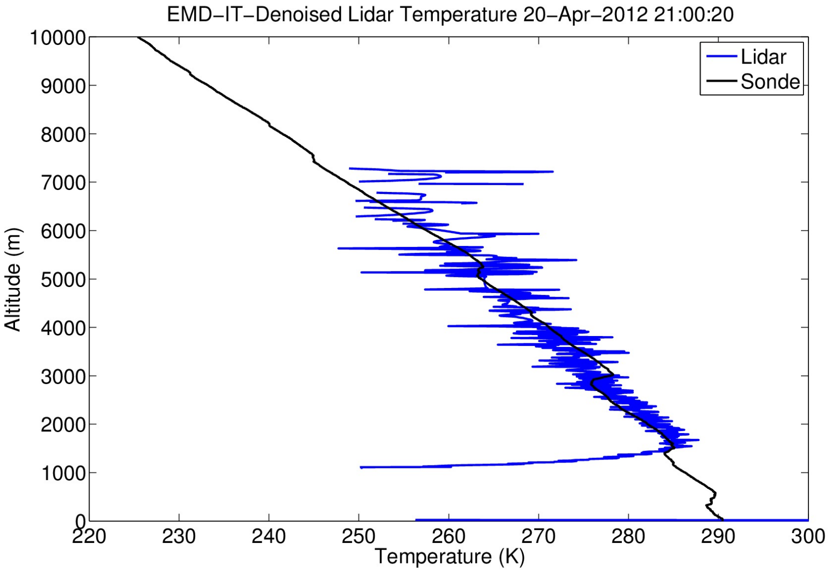

Results - 19–20 April 2012 Temperature

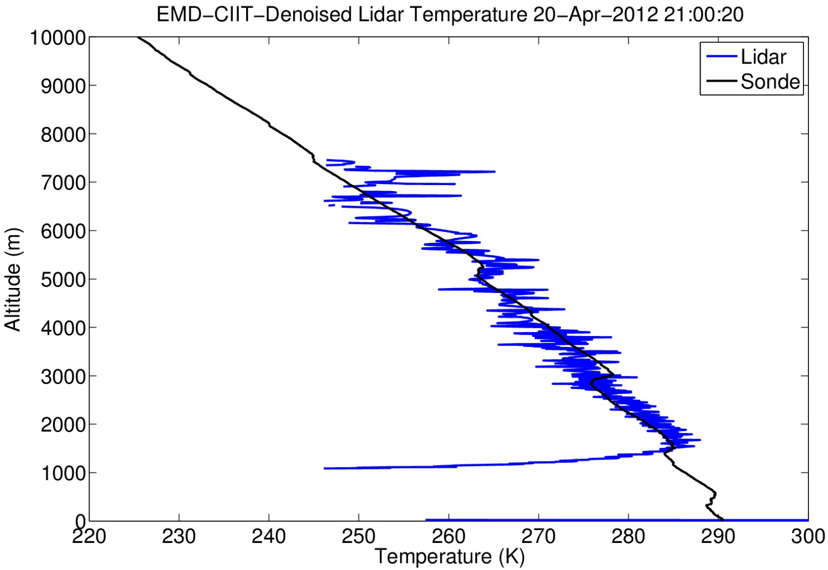

Results - 19–20 April 2012 Temperature

Noise-Reduction Statistics for Denoised Temperature Profiles Measured 19–20 April 2012

Method	20 April 2012, 00:00			20 April 2012, 21:00		
	σ_T	RMSE	r_T	σ_T	RMSE	r_T
Base	10.763	0.226	0.774	11.992	0.245	0.793
Avg15	10.062	0.117	0.951	9.839	0.103	0.965
Avg30	10.180	0.100	0.968	9.942	0.092	0.976
Avg60	10.117	0.085	0.978	9.773	0.071	0.985
DB4	10.026	0.101	0.959	10.064	0.104	0.967
DB6	9.936	0.104	0.959	9.979	0.098	0.968
DB8	10.130	0.104	0.962	9.882	0.104	0.960
IT	10.280	0.143	0.934	10.167	0.137	0.925
CIIT	10.242	0.114	0.958	10.107	0.111	0.962

Results - 21 April 2012 PBL Heights

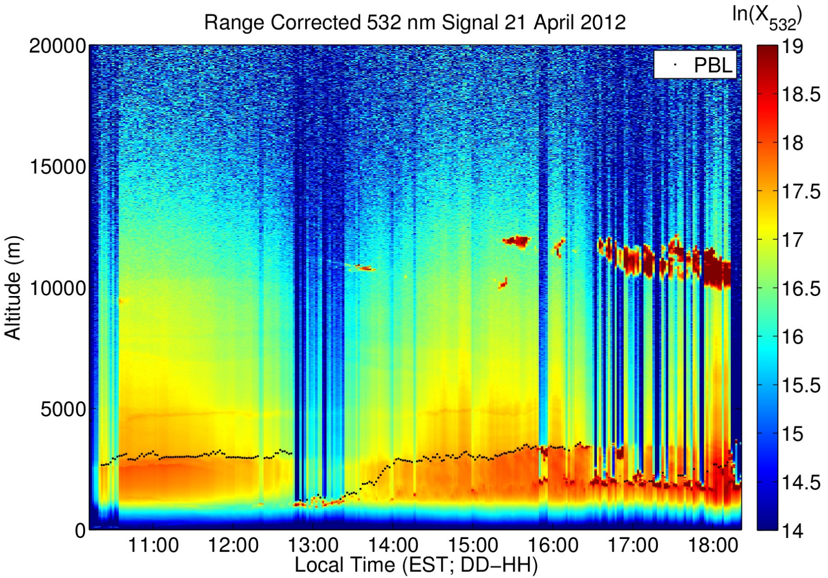

Results - 21 April 2012 PBL Heights

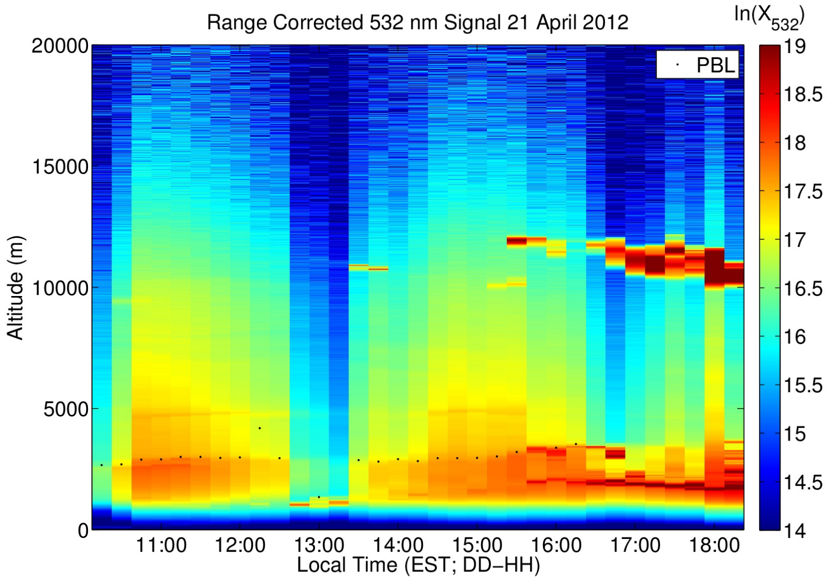

Results - 21 April 2012 PBL Heights

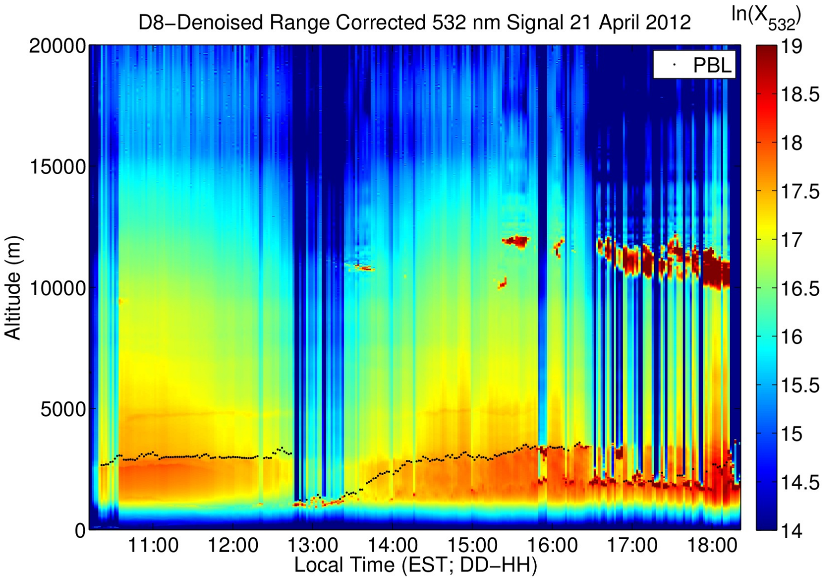

Results - 21 April 2012 PBL Heights

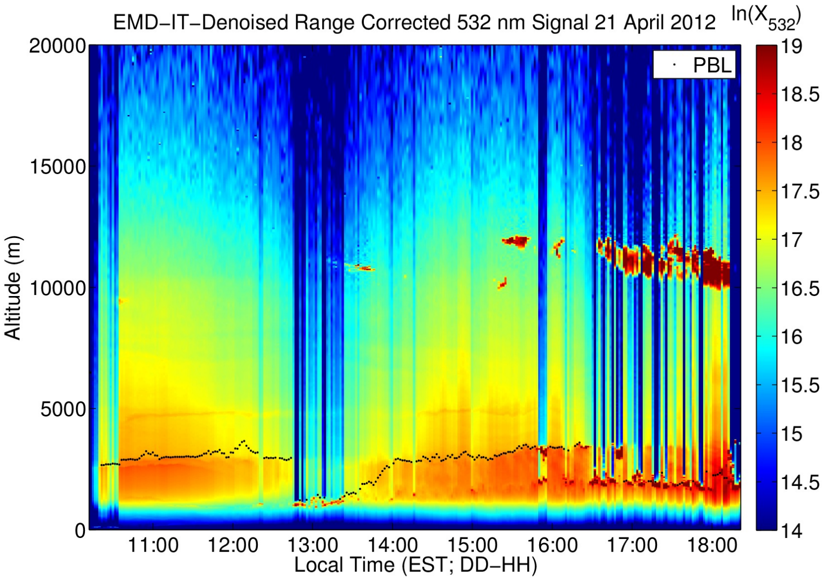

Results - 21 April 2012 PBL Heights

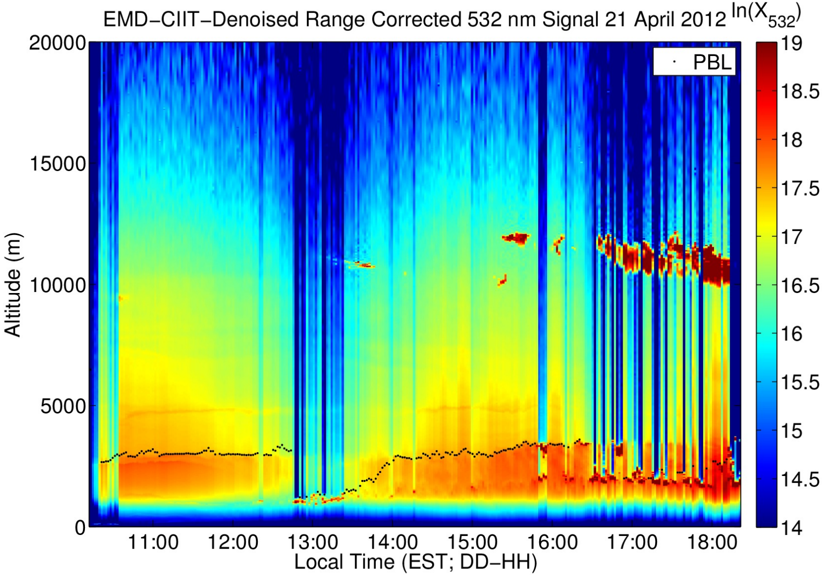

Results - 21 April 2012 PBL Heights